

RSC Advances



This is an *Accepted Manuscript*, which has been through the Royal Society of Chemistry peer review process and has been accepted for publication.

Accepted Manuscripts are published online shortly after acceptance, before technical editing, formatting and proof reading. Using this free service, authors can make their results available to the community, in citable form, before we publish the edited article. This *Accepted Manuscript* will be replaced by the edited, formatted and paginated article as soon as this is available.

You can find more information about *Accepted Manuscripts* in the [Information for Authors](#).

Please note that technical editing may introduce minor changes to the text and/or graphics, which may alter content. The journal's standard [Terms & Conditions](#) and the [Ethical guidelines](#) still apply. In no event shall the Royal Society of Chemistry be held responsible for any errors or omissions in this *Accepted Manuscript* or any consequences arising from the use of any information it contains.

Plasmo-optoelectronic tuning of optical properties and SERS response of ordered silver grating by free carrier generation

Y. Kalachyova,^a D. Alkhimova,^a M. Kostejn,^b P. Machac,^a V. Svorcik,^a O. Lyutakov^{a,*}

^a Department of Solid State Engineering, University of Chemistry and Technology, 16628 Prague, Czech Republic

^b Institute of Chemical Process Fundamentals, Academy of Sciences of the Czech Republic, 16502 Prague, Czech Republic

Abstract

Electrical current induced reversible tuning of the optical properties of ordered silver gratings was proposed. Polymer surface was patterned by excimer laser leading to creation of grating. Subsequently, thin silver layer was deposited onto the polymer grating. Prepared structure is capable of supporting surface plasmon polariton excitation and propagation. To introduce an electric current in direction along the features of the grating additional contacts (Au, Ag, Si, Ge, and their combination) were vacuum deposited. Application of the electric voltage leads to the shift of the wavelength position of surface plasmon polariton by several nanometers and to a change of its absolute intensity by up to 30 % in regard to its initial value. The observed phenomenon depends strongly on the grating amplitude and contact between the silver grating and the supply electrodes. The strong electric triggering was observed in the case of evaporated silver or gold electrodes. Oppositely, when the semiconductor materials (Ge, Si) were used, no optoelectronic response was observed. The observed optical tuning can be attributed to a change of free electron concentration in the silver grating due to impact ionization of the metal atoms. The observed phenomenon was exploited to modify SERS response of a thin polystyrene layer deposited onto silver grating. Electrically triggered increase and decrease of SERS intensity was found to depend on grating structure and excitation wavelength. The studied phenomenon is dynamic, continuous, reversible and voltage-controlled, and has a broad range of potential applications for example in the field of triggerable plasmon structures.

*Corresponding author (O. Lyutakov): *E mail:* lyutakoo@vscht.cz

Introduction

One of the new generations of plasmonic optical devices will be based on „smart“ materials with tunable optical properties. Absorption and scattering phenomena in such materials must be externally triggerable, providing an additional degree of freedom in the design of optical component and enabling construction of prodigious devices, such as a sensor able to detect single-molecular event [1-3]. Building blocks for smart plasmonic materials are now represented by modified noble metal nanostructures or highly doped semiconductors [4, 5]. In the case of noble metals, optical response is well described by Drude free electron model (modified with interband electron transition terms):

$$\varepsilon = \varepsilon' + i\varepsilon'' = \varepsilon_\infty - \frac{\omega_p^2}{\omega^2 + \Gamma^2} + i \frac{\omega_p^2 \Gamma}{\omega(\omega^2 + \Gamma^2)}, \quad (1)$$

where ω_p is plasma frequency determined by the conductive electron concentration (n) and the electron effective mass (m), ε is dielectric constant (ε' and ε'' – real and imaginary component of ε) and Γ is damping constant, which includes spatial confinement of free electrons by the nanoobject geometrical boundaries (R) [6, 7]:

$$\omega_p = \sqrt{\frac{ne^2}{\varepsilon_0 m}}, \quad (2)$$

$$\Gamma = \Gamma_{bulk} + a \frac{V_f}{R}. \quad (3)$$

In turn, position and height of plasmon absorption peak is determined by the interplay of metal and surrounding medium dielectric functions (ε_m). In the case of well separated nanoparticles (NPs) extinction coefficient achieves maximum value when [6]:

$$\varepsilon' \cong -2\varepsilon_m \text{ and } \varepsilon'' \rightarrow 0 \text{ or } \varepsilon'' \neq f(\omega). \quad (4)$$

For large NPs or closed-packed array of NPs the extinction coefficient is affected by higher-order multipole absorption and adequate description of resonance conditions requires more general equations (4). However, the situation remains similar in principle – position and intensity of plasmon-related absorption depend on the interplay of metal and surrounding medium dielectric functions.

A usual way of the plasmon absorption tuning is changing of geometrical boundaries of the nanoobject through changing the shape and size of the NPs (i.e. the term R in the Eq. (3)). This affects the damping constant and metal dielectric function in Eq. (1) [8-10]. This approach means irreversible setting of the plasmon resonance once and forever. Alternatively, dielectric function of surrounding medium can be reversibly affected (i.e. the term ε_m in the Eq. (4)) which leads to modification of the strength and position of the plasmon resonance peak [11, 12]. As an example,

the reversible formation and dissolution of Ag₂O nanoshells around Ag nanoclusters was proposed [13]. Some interesting examples of this approach are application of electrically triggerable liquid crystal coatings (electrical tuning) and modification of surface of the metal NPs with smart polymers (pH or temperature tuning) [14-17]. Electrical field was also applied to induce heating of substrates supporting the NPs or phase transition in dielectric medium nearby the NPs followed by shift of plasmon peak [18, 19].

However, in the Eq. (2) there is another term, which can be modified – the free electron concentration. Modification of electron densities (n) in the AuNPs was theoretically calculated in [20] by substitution of n by n_s in Eq. (2), where n_s is the state dependent variable. It has been shown that an increase of the free electron density of an isolated nanostructure leads to a blue shift, while a decrease of the free electron density leads to a red shift of the plasmon resonance peak. From the experimental point of view the free electron concentration was changed by introduction of chemical reducing agents or immobilization of the metal NPs on charged electrodes [3]. In the latter case, application of electrical voltage caused an injection/drain of electrons into/from the NPs [21]. Alternatively, metal NPs were charged by argon plasma or by electron beam [22, 23]. Variation of the charging effect with NPs shape and size was observed as well [24]. Generally, the plasmon peak does not shift more than 1-10 nm and its intensity increases up to several percent in regard to the initial value. On the other hand, changes of the plasmonic properties can be even more significant in the case of coupled nanostructures [25], which open a way for a practical utilization of the plasmoelectronic effect.

In this paper we propose an alternative approach for changing of free electron density and control of plasmonic response of nanostructures. In contrast to published studies we modified the concentration of free electrons in surface plasmon-polariton supported silver structures through free carrier generation by impact ionization on the metal nanostructures/bulk metal interface. The surface morphology of PMMA and the metal grating was examined by AFM technique. Properties of the prepared structures were characterized by UV-Vis and Raman spectroscopy and electrical measurements.

Experimental

Materials

Polymethylmethacrylate (PMMA, $M_w \sim 1,500$ K) of optical purity was supplied by Goodfellow Inc., Fast Red ITR of 96 % grade ($\lambda_{\text{abs}}^{\text{max}} = 226$ nm) was purchased from Sigma-Aldrich. Glass substrates were provided by Glassbel Ltd., CZ. Polystyrene (PS) was supplied by

Goodfellow Inc. and dissolved in toluene (LachNer, Czech Republic). Silver target (99.99 % of purity) was purchased from Safina CZ.

Sample preparation

The Fast Red (FR)-doped PMMA films were prepared by separate dissolving the PMMA and the Fast Red ITR in 1,2-dichloroethane. Then, 7.0 wt. % PMMA and 2.8 wt. % FR solutions were mixed and spin-coated onto freshly cleaned glass substrates. The prepared samples were dried under ambient conditions for 24 h. Then samples were irradiated with KrF excimer pulse laser (40 ns, $\lambda = 248$ nm) at a repetition rate of 10 Hz (Lambda Physik COMPexPro 50, Coherent Inc., Göttingen, Germany). The laser beam was polarized linearly with a cube of UV-grade fused silica with an active polarization layer. The samples were irradiated with 150, 170 and 190 laser pulses with laser fluency of 12 mJ cm^{-2} . Incidence angle of the laser beam with respect to the sample surface normal was 50° and aperture with area of $5 \times 10 \text{ mm}^2$ was used. As a result, periodic surface structures were created on the PMMA surface [12, 26]. Gratings with different periodicities was prepared by changing the laser beam incidence angle. Close to normal incidence angles lead to creation of the gratings with the wavelength close to the laser light wavelength (270 nm); by increasing the incidence angle to 30° and 50° the gratings with the wavelengths 350 and 450 nm respectively were created [27].

Silver was then deposited onto the patterned surface by vacuum sputtering method (DC Ar plasma, gas purity 99.995 %, gas pressure of 4 Pa, discharge power of 7.5 W, sputtering time 100, 200, and 300 s.). Polystyrene (PS) thin film was prepared by dropping 0.5 wt. % PS solution onto the prepared surface at a spin rate of 1200 rpm for 5 s.

The contacts were prepared in a vacuum deposition apparatus UNIVEX 450. The thickness of the prepared contacts was controlled by a calibrated crystal gauge. The depositions were performed under following conditions: Au - 100 nm, thermal evaporation from speed of deposition 0,5 nm/s; Ag – thickness 100 nm, thermal evaporation from speed of deposition 0,3 nm/s; Ge – thickness 100 nm, evaporation using electron gun, speed of deposition 0,1 nm/s. The initial pressure was $2 \cdot 10^{-6}$ mbar in all cases and the substrate was kept at room temperature. The purity of the deposited materials was 4N. The thickness of the prepared contacts was controlled by a calibrated crystal gauge.

Diagnostic methods

The surface morphology of PMMA and the grating structures was examined with an AFM technique using a VEECO CP II device ('tapping' mode, probe RTESPA-CP, spring constant $50 \text{ N} \cdot \text{m}^{-1}$, Veeco Instruments Inc., USA). UV-Vis absorption spectra were measured using PerkinElmer's Lambda 25 UV/Vis/NIR Spectrometer in the spectral range of 300-1100 nm at a

scanning rate of $240 \text{ nm} \cdot \text{min}^{-1}$ and a data collection interval of 1 nm. Electrical measurements were realized using E3631A DC Power Supply (Agilent, USA). Raman scattering was measured on Nicolet Almega XR spectrometer (Laser power 15 mW) with 470 and 785 nm excitation wavelength. Spectra were measured 10 times, each of them with 30 s accumulation time.

Results and Discussion

It was initially proposed that an electric triggering of regular silver grating can change the optical response of ordered metal nanostructure and tune the surface plasmon-polariton excitation. To verify this hypothesis several sets of experiments were performed: (i) investigation of the dependences of optical properties on the applied voltage and current with respect to the volt-ampere characteristic of the structure, (ii) taking into account the grating amplitude and periodicity and the effect of the materials used to introduce the electric current. Schematic representation of experimental set-up is shown in Fig. 1. In particular, thin layer of Ag was sputtered onto previously patterned PMMA surface and equipped with two electrodes for introduction of the electric current in a direction parallel to the grating. The applied voltage varied in the range of 0-17 V. The gratings were prepared with periodicity of 270-450 nm and amplitude of 10-50 nm. As material for the electrodes different combinations of silver, gold, silicon and germanium were tested.

To create gratings with different amplitudes, different numbers of laser pulses were used at a constant angle of incidence and laser flow. Surface morphology of the patterned polymer surfaces is presented in Fig. 2. Application of 120, 150 and 190 laser pulses leads to a gradual decrease of grating amplitude from 50 to 10 nm. After the laser modification the patterned surfaces were coated with a sputtered silver layer (effective thickness 30 nm) [28]. The created structure is expected to support surface plasmon polariton (SPP) excitation under illumination with light of a certain wavelength. Effectivity and optimal wavelength of the SPP excitation depends strongly on the grating amplitude [29]. With increasing grating amplitude “red shift” of optimal SPP excitation wavelength is expected as well as more effective SPP excitation.

Surface topographies of the gratings after silver sputtering are shown in the Fig. 3 for the deposition times 100 (Fig. 3A), 200 (Fig. 3B) and 300 s (Fig. 3C) . It is evident, that the initial grating structure is conserved during the sputtering. Slight increase in the grating amplitude can be attributed to predominant silver deposition onto tops of surface features. An increase of nano-roughness due to the formation of silver clusters is evident too. For further experiments the silver layer formed after 100 s of sputtering time (Ag layer 25-30 nm thick) was chosen because it shows maximal SERS response from both, the theoretical and experimental points of view as was shown in our previous work [29].

The silver grating UV-Vis absorption spectra obtained with and without electric current are presented in Fig. 4. Applying an electric field of an above critical value (7-11 V in this case) induces significant changes in the optical properties of the silver grating. Each spectrum can be divided into two parts: (i) longer wavelengths, where absorption decreases with increasing voltage and (ii) shorter wavelengths, where absorption increases. Areas of transition between the longer and shorter wavelengths are highlighted by dashed squares. Their position depends strongly on the grating amplitude (see Fig. 4). Arrows in the graphs suggest the direction in which the absorption is shifted with increasing voltage. The transition areas are red-shifted with decreasing grating amplitude. In each spectrum the position of the SPP absorption peak is evident. As can be expected, the SPP peak position is red-shifted with increasing grating periodicity. On the other hand, position of the SPP peak depends only slightly on the applied voltage. The SPP is blue-shifted by cca 8 nm with increasing voltage. A similar slight shift of absorption maximum position was theoretically and experimentally reported for the case of localized surface plasmon (LSP) resonance [20-24]. But unlike in the case of LSP, the reported shift of SPP is accompanied by significant changes of absolute absorption coefficient at the SPP peak wavelength. Depending on the position of the transition area, SPP peak is located in the shorter or longer wavelength part of the spectrum and correspondingly its absolute value of absorption decreases or increases by cca 30 %.

On gratings with lower amplitudes more homogenous silver layers are formed. With increasing grating amplitude the thickness of the silver layer becomes more modulated, due to the higher surface roughness and preferential silver deposition on the tops of grating. In the highly modulated silver layer the electron gas is better confined, comparing with that in the homogenous layer. Thus quantum-related phenomena, such as electron scattering events and impact ionization of silver atoms become more pronounced. This fact is reflected in greater changes in the optical spectra in the case of grating with 57 nm amplitude (the Fig. 4) or in the shift of transition area to longer wavelength with the amplitude decrease.

The influence of the grating periodicity on the observed optoelectronic phenomenon was also evaluated. Unlike in the previous case, changes of the grating periodicity do not lead to apparent changes of the optical properties of the structure. Similarly to the previous case each structure exhibits shorter and longer wavelength parts of spectrum, but position of the transition area does not shift with changing periodicity.

Evaluation of silver grating – bulk contact interface was performed as well. Metals (Au and Ag) and semiconductors (Ge and Si) were used as contact materials. After the deposition process conductivity of all the structures was checked to have similar values. In the case of the semiconductor materials no optoelectronic effect was observed. On the other hand, different

combinations of metals not only supported appearance of the optoelectronic effect, but also affected its pattern. Absorption spectra corresponding to Au-Au, Au-Ag, and Ag-Ag metal contacts are represented in Fig. 5. The main difference between metals and semiconductors is the presence of a band gap, which restricts the concentration of free electrons. We can therefore conclude that the optoelectronic phenomenon in silver grating can be initiated only when it is in contact with materials with high free electron density. It is also evident, that Au, which has a slightly higher concentration of free electrons compared to Ag, produces slightly large changes of the optical response.

Increase of free electron concentration can be estimated from the shift of SPP position. The condition of SPP excitation on the grating is given by following equation:

$$k_0 \sin \theta = k_{spp} - q \frac{2\pi}{\Lambda} \quad (5)$$

where the k_0 and k_{spp} are the wave numbers of incident and surface plasmon polariton waves, θ is the angle of light incidence, Λ is the grating periodicity and q is the whole, positive number. For the SPP excitation by the perpendicular light illumination and for first order of SPP excitation eq. 5 can be simplified:

$$k_{spp} = \frac{2\pi}{\lambda} + \frac{2\pi}{\Lambda} = \frac{\omega_{spp}}{c} \quad (6)$$

and the frequency of excited SPPs can be calculated. Taking into account that the surface plasma frequency is given by:

$$\omega_{spp} = \frac{\omega_p}{\sqrt{2}} = \sqrt{\frac{ne^2}{2\varepsilon_0 m}} \quad (7)$$

the increase of free electron concentration under applied voltage can be calculated as follow (with known ω_{spp} from Eq. 6):

$$\Delta n = \frac{2\varepsilon_0 m ((\omega_{spp}^{(2)})^2 - (\omega_{spp}^{(1)})^2)}{e^2} \quad (8)$$

where the $(\omega_{spp}^{(2)})$ and $(\omega_{spp}^{(1)})$ are the asymptotic values of SPPs frequencies with and without application of voltage. Results obtained in this way are summarized in the Tab. 1A for different grating amplitudes and in the Tab. 1B for different metal contacts.

From the calculated data in the Tab. 1 is evident, that the free carrier concentration increases when external voltage is applied. This phenomenon is not apparent for low voltages but it becomes noticeable after exceeding a certain critical voltage. The absolute value of free carrier changes (10^{26}) constitutes approximately one percent of the total concentration of free carriers in silver (10^{28}). This result corresponds well with the results published for LSP case [3, 21, 22], where the increasing of free carrier concentration by one percent leads to similar changes in the plasmon absorption peak. From the Tab. 1A is evident, that the calculated changes of free carries slightly

increase with decreasing of grating amplitude but the observed differences are of the order of the errors introduced by the simplified model chosen for calculation. The second part of Tab. 1 shows the effect of contact metals on the changes in the free carrier concentration. In this case only slight differences between Ag-Ag and Au-Au contacts were found. This fact can be explained by the likeness between the electronic band gap constants of Ag and Au.

The observed phenomena were applied to tune the SERS response of silver grating (see Fig. 5). Of all the prepared grating-contact combinations, the structure shown in Fig. 5B was chosen, because it exhibits the most significant increase of the SPP peak induced by the increasing voltage. Two wavelengths were used for the SERS probes – 470 and 785 nm – corresponding to near UV and near IR part of optical spectrum. Voltage-dependent absorption coefficients at a mean wavelength and volt-ampere (VA) characteristic of the silver grating are shown in Fig. 6. On the VA curve two areas are apparent: area of ohmic behavior, where an increase of applied voltage leads to a proportional increase of electric current and a second area, where the VA curve deviates from the linear ohmic behavior. In the latter case the applied voltage induces greater current than expected. Absorption coefficients show voltage dependence as well, which perfectly corresponds to the VA characteristic. In the ohmic part of the dependence, absorption coefficients remain constant. With the deviation from ohmic behavior, absorption coefficients change rapidly when the voltage further increases – the absorption at 475 nm increases and absorption at 785 nm decreases. Initial increase of the absorption coefficient at 785 nm lies within attributed measuring error but it could also be due to thermal heating of silver layer by electric current which can lead to an increase in the reflectivity of Ag in the near IR area and a seeming increase in the absorption coefficient as well.

Effects of silver thickness on the changes of absorption coefficients at the 470 nm and 785 nm were also estimated and presented in the Fig. 7 for 200 and 300 s Ag sputtering times. Increasing of sputtering time corresponds to proportional increase of silver thickness by a factors 2 and 3 compared to the Fig. 6. The precise thickness of Ag film is not given because the metal does not form the homogeneous layer on the patterned polymer surface. From the Fig. 6A, 6B and the Fig. 7 is evident, that increasing of the silver film thickness leads to the greater absorption coefficient at the both wavelength (as can be expected), but the voltage induced changes of absorption coefficients become smaller. This effect can be expected, because with the increasing film thickness the silver tends to achieve the “bulk” electronic structure, and the free carrier generation becomes more hampered.

SERS measurements were performed using an additional thin layer of polystyrene (PS) on the silver grating. PS was chosen as a typical SERS analyte which remains stable and produces a well defined SERS signal. Additionally, PS allows preventing photo and photothermal degradation.

Results of the SERS measurements are plotted in Fig. 8. The inset shows a typical curve from which intensity of the stronger Raman scattering peak located at 1000 cm^{-1} was used as a marker of the enhancement. Intensity of this peak was plotted against the applied voltage in the main part of Fig. 8. In both 470 and 785 nm Raman excitation wavelengths strong voltage dependences were found. In the case of the excitation wavelength of 470 nm the SERS signal increases and reaches almost triple the initial value. Opposite situation occurs in the case of excitation by 785 nm - the intensity of SERS decreases with increasing voltage and achieves ca 50 % of the initial value. The results of SERS measurements correspond well with the absorption measurements “in-principle” - an increase of absorption leads to an increase of SERS signal and vice versa. As to the particular shape of the curves, some discrepancy can be found – unlike the absorption coefficients, the SERS intensity increases even at low voltages. This difference can be attributed to a local effect in the laser illuminated spot, where electrical current and laser treatment work together.

Test of reversibility of the observed optical properties and surface enhancement phenomenon tuning was performed by application of an alternating electric field (15 V). The results for sample with 30 nm grating amplitude and Au electrodes are presented in Fig. 9. It shows the changes are reversible in both cases, application of the alternating field leads to an increase of SERS intensity and absorption coefficient at 470 nm. The observed process remains stable up to fifteen cycles in most cases. A slow decrease of effectivity of the tuning process was observed after that, probably due to structure degradation. Relaxation time was found to be lower than measurement limit (1 s). This indicates that the optical tuning can be attributed rather to the impact mechanism induced changes of free electron density, than to a thermal excitation.

An attempt to explain the observed phenomenon was made. The following points are key to understand the nature of the phenomenon: (i) silver grating exhibits apparent optoelectronic response, (ii) appearance of optical response depends on the material of contact attached to the grating and the amplitude of the grating, (iii) the optoelectronic phenomenon does not depend on the grating periodicity, and (iv) the optoelectronic phenomenon did not appear when semiconductor contacts were employed despite the fact the electric current and voltage were similar to the case of metal contacts. With all of the above in mind we suggest the process is based on an increase of free electron density in the silver nanostructures due to forced ionization of the Ag atoms. Impact ionization occurs due to thermal or hammer mechanism. Strong dependence on the material of contacts indicates the hammer mechanism is more dominant. In different words: applied external voltage forces the electrons to move from bulk metal to the silver grating. At a certain critical voltage the electrons gain enough energy for the ionization of the Ag atoms, which leads to an increase of free electron density. This system can be compared to a Zener diode near a breakdown

voltage. Proposed mechanism also explains the existence of critical voltage, beyond which apparent changes in the optical spectra occurs. Electrons need to have certain energy to induce the impact ionization of silver atoms and generation of free carriers. This energy is a function of applied voltage, and above a critical voltage non-linear increase of electric current and abrupt changes of optical properties due to impact ionization of silver atoms take place. Below of the critical voltage silver ionization does not occur and optical spectra as well as electrical response remain constant.

Conclusion

Optoelectronic tuning of plasmonic properties of ordered silver grating was reported. Application of an external stimulus (voltage) initiates an increase of free electron concentration in silver by impact ionization mechanism. As a result a slight shift of surface plasmon polariton wavelength position and strong changes of its intensity were observed. The observed effects were found to be dependent on parameters of the grating – its amplitude and the silver/contact interface. This phenomenon was also exploited to control SERS properties of the silver grating, which is related to the surface plasmon polariton excitation. The studied changes were found to be reversible and can find application in the field of smart plasmonics and tunable surface-related applications.

Acknowledgement

This work was supported by the GACR under the projects 15-19209S, 15-19485S and by the TACR under the project TA04021007.

References

- 1 S. Rehwald, S. M. Berndt, F. Katzenberg, S. Schwieger, E. Runge, K. Schierbaum and D. Zerulla, *Phys. Rev. B.*, 2007, **76**, 085420.
- 2 A. Tittl, X. H. Yin, H. Giessen, X. D. Tian, Z. Q. Tian, C. Kremers, D. N. Chigrin and N. Liu, *Nano Lett.* 2013, **13**, 1816-1821.
- 3 C. Novo, A. M. Funston, A. K. Gooding and P. Mulvaney, *J. Am. Chem. Soc.* 2009, **131**, 14664–14666.
- 4 J. M. Luther, P. K. Jain, T. Ewers and A. P. Alivisatos, *Nature Mater.* 2011, **10**, 361-366.
- 5 P. A. Kossyrev, A. Yin, S. G. Cloutier, D. A. Cardimona, D. Huang, P. M. Alsing and J. M. Xu, *Nano Lett.*, 2005, **5**, 1978-1981.
- 6 S. A. Maier, *Springer*, 2007.
- 7 K. L. Kelly, E. Coronado, L. L. Zhao, and G. C. Schatz, *J. Phys. Chem. B* 2003, **107**, 668-677.

- 8 P. K. Jain, K. S. Lee, I. H. El-Sayed and M. A. El-Sayed, *J. Phys. Chem. B*, 2006, **110**, 7238-7248.
- 9 M. A. El-Sayed, *Accounts Chem. Res.*, 2001, **34**, 257-264.
- 10 Y. K. Mishra, S. Mohapatra, R. Singhal, D. K. Avasthi, D. C. Agarwal, and S. B. Ogale, *Appl. Phys. Lett.*, 2008, **92**, 043107.
- 11 T. R. Jensen, M. D. Malinsky, C. L. Haynes, and R. P. Van Duyne, *J. Phys. Chem. B* 2000, **104**, 10549-10556.
- 12 Y. Kalachyova, O. Lyutakov, P. Slepicka, R. Elashnikov and V. Svorcik, *Nanoscale Res. Lett.*, 2014, **9**, 591.
- 13 S. Mohapatra, *J. Alloy. Compd.*, 2014, **598**, 11-15.
- 14 S. Volden, A. L. Kjoniksen, K. Z. Zhu, J. Genzer, B. Nystrom and W. R. Glomm, *ACS Nano*, 2010, **4**, 1187-1201.
- 15 P. Tian, Q. L. Wu and K. Lian, *J. Appl. Polym. Sci.*, 2008, **108**, 2226-2232.
- 16 X. Qian, J. Li and S. Nie, *J. Am. Chem. Soc.*, 2009, **131**, 7540-7541.
- 17 K. C. Chu, C. Y. Chao, Y. F. Chen, Y. C. Wu and C. C. Chen, *Appl. Phys. Lett.*, 2006, **89**, 103107.
- 18 E. A. Shaner, J. G. Cederberg and D. Wasserman, *Appl. Phys. Lett.*, 2007, **91**, 181110.
- 19 T. Driscoll, H.-T. Kim, B.-G. Chae, B.-J. Kim, Y.-W. Lee, N. M. Jokerst, S. Palit, D. R. Smith and M. D. Ventra, D. N. Basov, *Science*, 2009, **325**, 1518-1521.
- 20 A. M. Brown, M. T. Sheldon and H. A. Atwater, *ACS Photonics* 2015, **2**, 459-464.
- 21 G. Garcia, R. Buonsanti, E. L. Runnerstrom, R. J. Mendelsberg, A. Llordes, A. Anders, T. J. Richardson and D. J. Milliron, *Nano Lett.* 2011, **11**, 4415-4420.
- 22 Y. Saito and K. Fujita, *Appl. Phys. Express* 2015, **8**, 015001.
- 23 M. I. Lapsley, A. Shahravan, Q. Hao, B. K. Juluri, S. Giardinelli, M. Lu, Y. Zhao, I.-K. Chiang, T. Matsoukas and T. J. Huang, *Appl. Phys. Lett.*, 2012, **100**, 101903.
- 24 B. K. Juluri, Y. B. Zheng, D. Ahmed, L. Jensen and T. J. Huang, *J. Phys. Chem. C* 2008, **112**, 7309-7317.
- 25 C. Liow, F. Meng, X. Chen and S. Li, *J. Phys. Chem. C* 2014, **118**, 27531-27538.
- 26 Y. Kalachyova, O. Lyutakov, M. Kostejn, M. Clupek and V. Svorcik, *Electron. Mater. Lett.* 2015, **11**, 288-294.
- 27 D. W. Bauerle, in *Laser Processing and Chemistry*, Springer, Berlin: 2011.
- 28 I. R. Hooper and J. R. Sambles, *Phys. Rev. B*, 2003, **67**, 235404.
- 29 Y. Kalachyova, D. Mares, O. Lyutakov, M. Kostejn, L. Lapcak and V. Svorcik, *Phys. Chem. C*, 2015, **119**, 9506-9512.

Tab. 1 Dependence of free carrier concentration changes on the applied voltage for different amplitudes of silver grating (A) and for different metal contacts (B).

Part. A			Part. B			
Metal contacts	Voltage (V)	Δn (N/m ³)	Amplitude (nm)	Voltage (V)	Δn (N/m ³)	
Ag-Ag	0-5	0	57	0-5	0	
	7	$0.98 \cdot 10^{26}$		7	$1.07 \cdot 10^{26}$	
	10-11	$1.47 \cdot 10^{26}$		10	$1.43 \cdot 10^{26}$	
	12	$2.45 \cdot 10^{26}$		11	$1.79 \cdot 10^{26}$	
	13	$2.95 \cdot 10^{26}$		12	$2.15 \cdot 10^{26}$	
	14	$3.25 \cdot 10^{26}$		13	$2.51 \cdot 10^{26}$	
Au-Au	0-3	0	32	14	$2.79 \cdot 10^{26}$	
	5	$0.49 \cdot 10^{26}$		15-16	$2.88 \cdot 10^{26}$	
	6-7	$0.98 \cdot 10^{26}$		11	0-11	0
	8	$1.05 \cdot 10^{26}$			12	$0.51 \cdot 10^{26}$
	9-10	$1.10 \cdot 10^{26}$	13		$1.26 \cdot 10^{26}$	
	11	$1.25 \cdot 10^{26}$	14		$1.99 \cdot 10^{26}$	
	12	$1.97 \cdot 10^{26}$	15	$2.49 \cdot 10^{26}$		
	13	$2.96 \cdot 10^{26}$	16	$2.99 \cdot 10^{26}$		
14	$3.56 \cdot 10^{26}$					
Ag-Au	0-7	0				
	10	$1.01 \cdot 10^{26}$				
	11	$1.5 \cdot 10^{26}$				
	12	$2 \cdot 10^{26}$				
	13	$2.5 \cdot 10^{26}$				
	14	$3.21 \cdot 10^{26}$				

Figure caption**Fig. 1**

Schematic representation of an experimental set-up for electric triggering of regular metal grating on polymer surface.

Fig. 2

Surface morphology of polymer gratings prepared by the excimer laser irradiation with incidence angle of 50° from surface normal and with: A – 190, B – 150, and C – 120 pulses.

Fig. 3

Surface morphology of sputtered silver layer deposited onto patterned polymer surface during A – 100 s., B – 200 s., and C – 300 s.

Fig. 4

Dependence of UV-Vis absorption of polymer gratings with different amplitudes (A – 57 nm, B – 32 nm, C – 11 nm) on applied external voltage (0 to 16 V).

Fig. 5

Dependence of UV-Vis absorption of metal-polymer grating with different metal contacts (A – Ag-Ag, B – Au-Au, C – Ag-Au contacts) on applied external voltage (0 to 14 V) .

Fig. 6

Dependence of A, B – SERS enhancement and C – electric current (VA characteristic) on applied external voltage. SERS spectra were obtained using A – 470 and B – 785 nm excitation wavelength.

Fig. 7

Dependence of absorption coefficients (at $\lambda_{\text{abs}} = 785$ nm and 470 nm) on the applied voltage for different amounts of deposited silver (A, B – 200 s.; C, D – 300 s.).

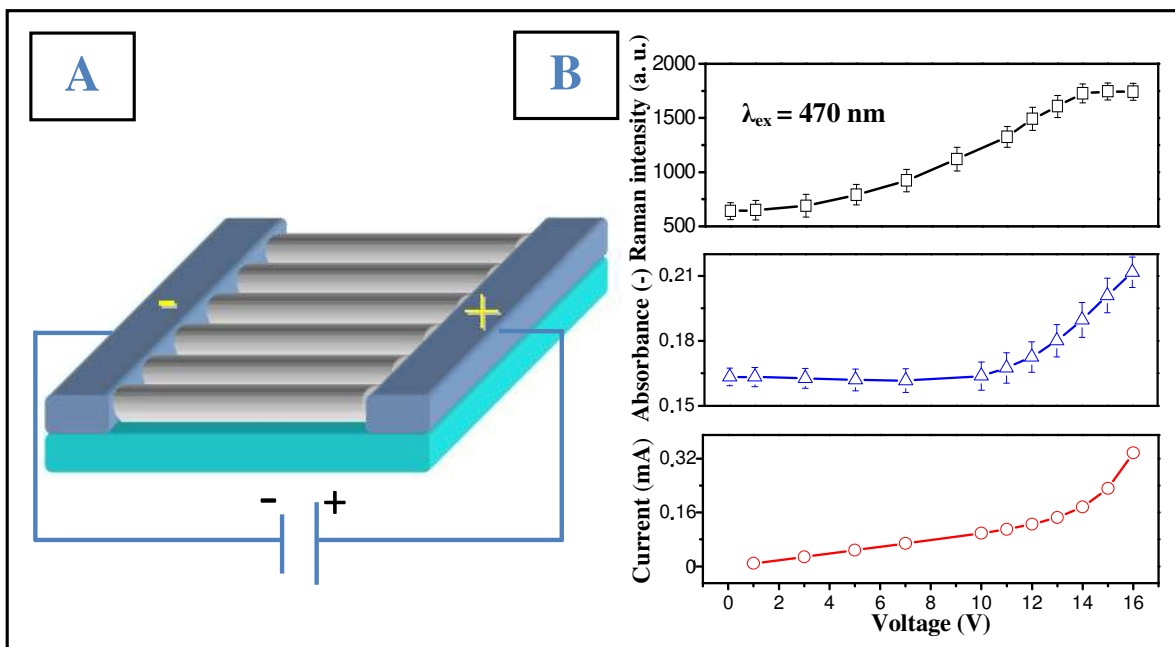
Fig 8

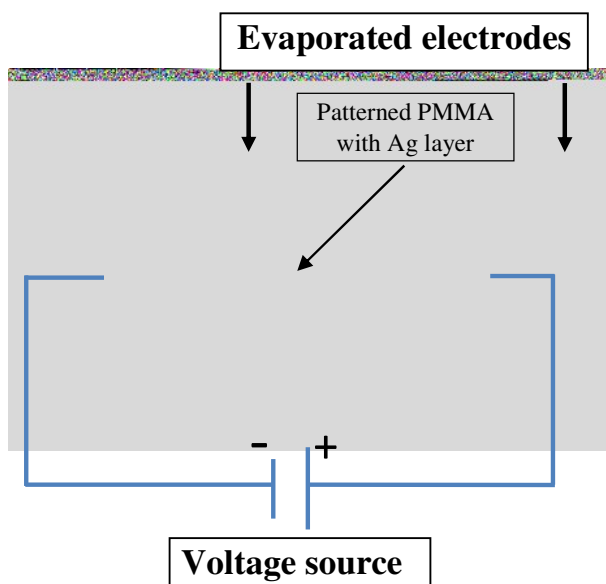
Dependence of maximum at 1000 cm^{-1} from Raman spectra (excitation wavelengths 470 and 785 nm) of silver grating on external voltage triggering. Characteristic Raman spectrum of PS excited by 470 nm in inset.

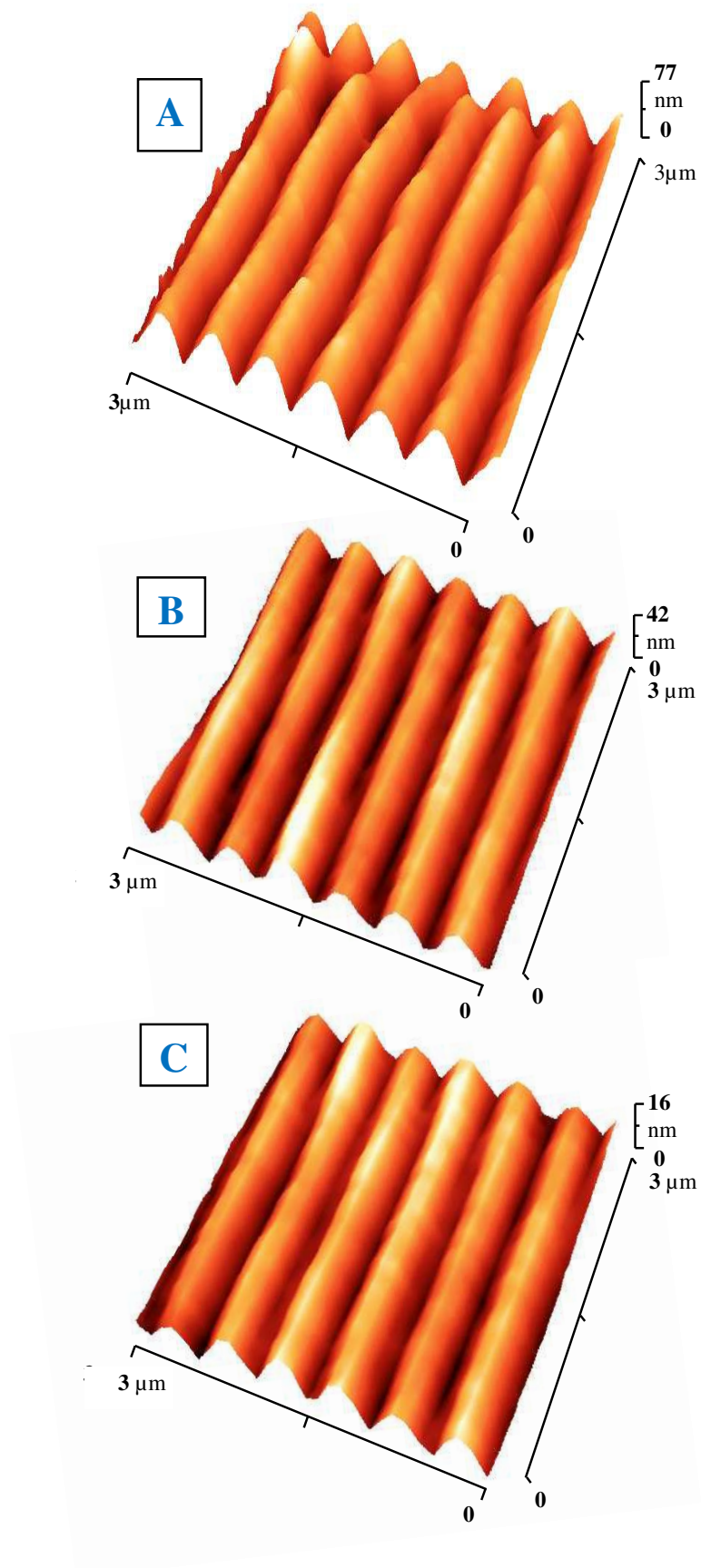
Fig. 9

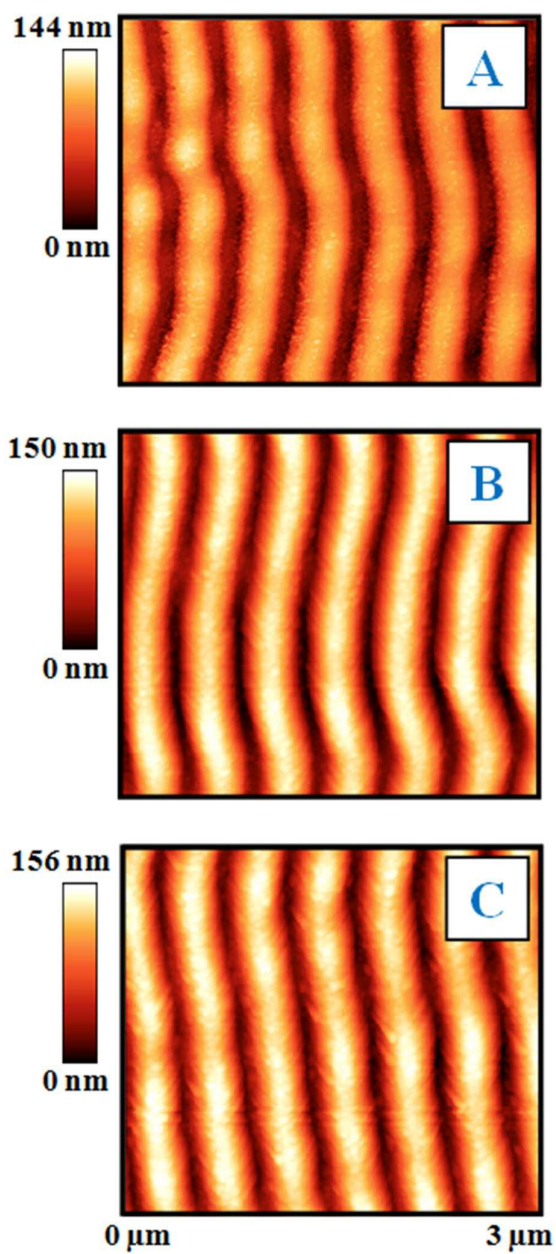
Reversibility test of SERS intensity (excited by 470 nm) and absorption coefficient at 470 nm modulation performed on the sample with 30 nm amplitude of grating, with thin silver layer. Electric current was repeatedly introduced to gold electrodes.

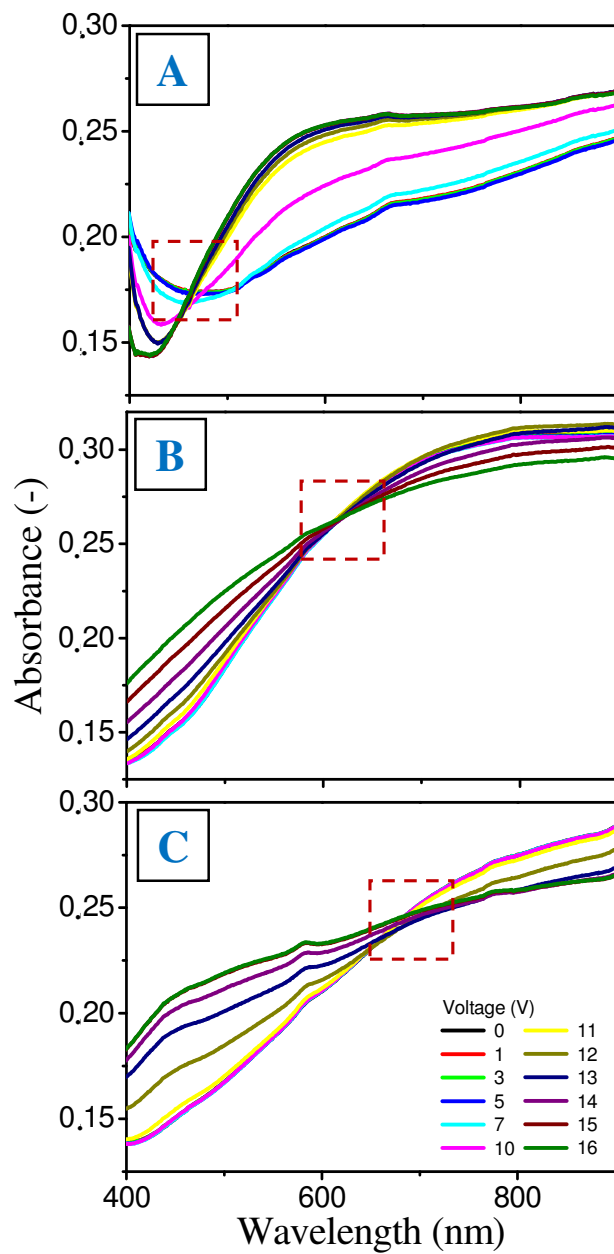
Graphical Abstract



**Fig. 1**

**Fig. 2**

**Fig. 3**

**Fig. 4**

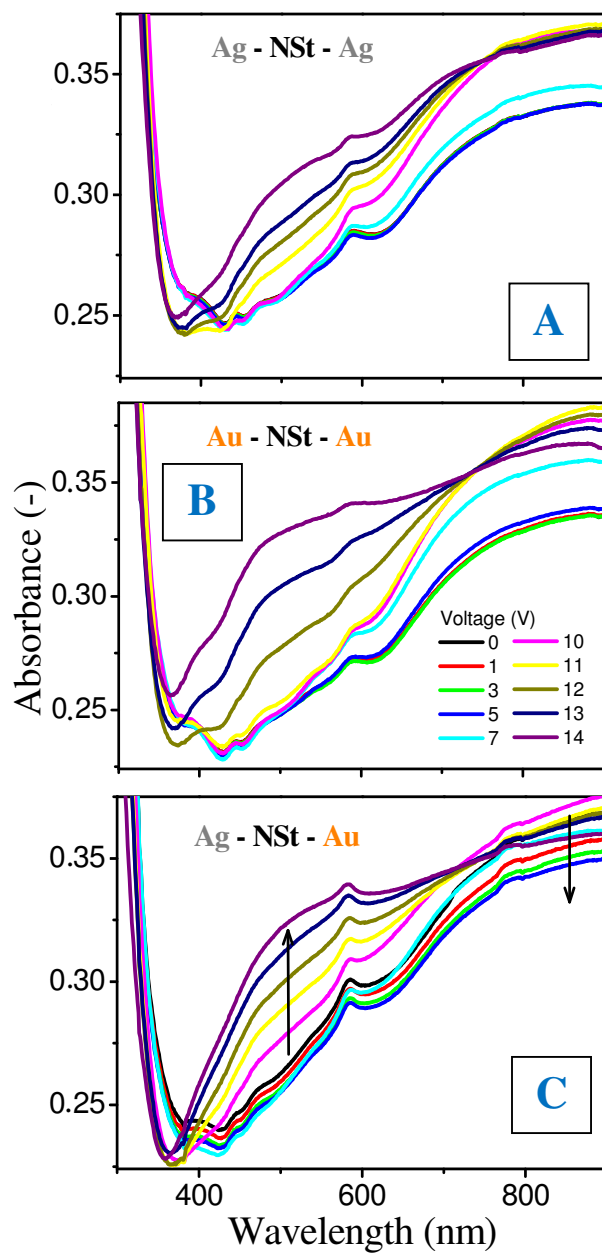


Fig. 5

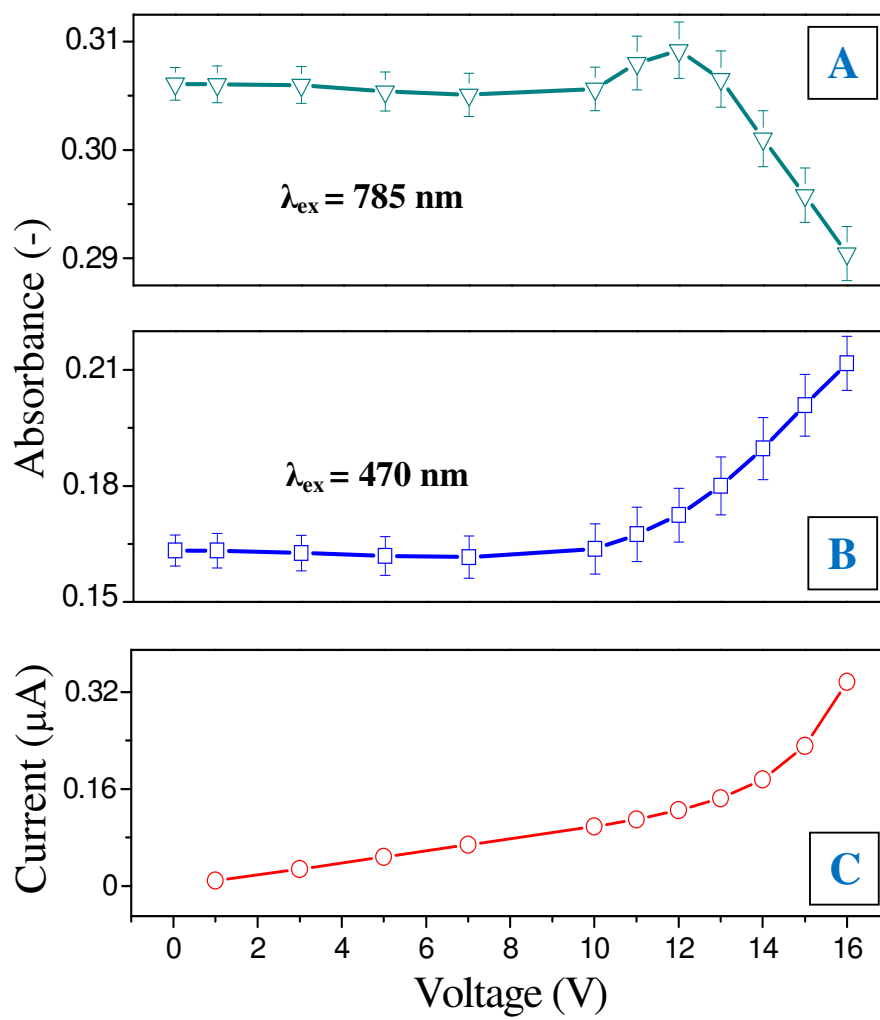
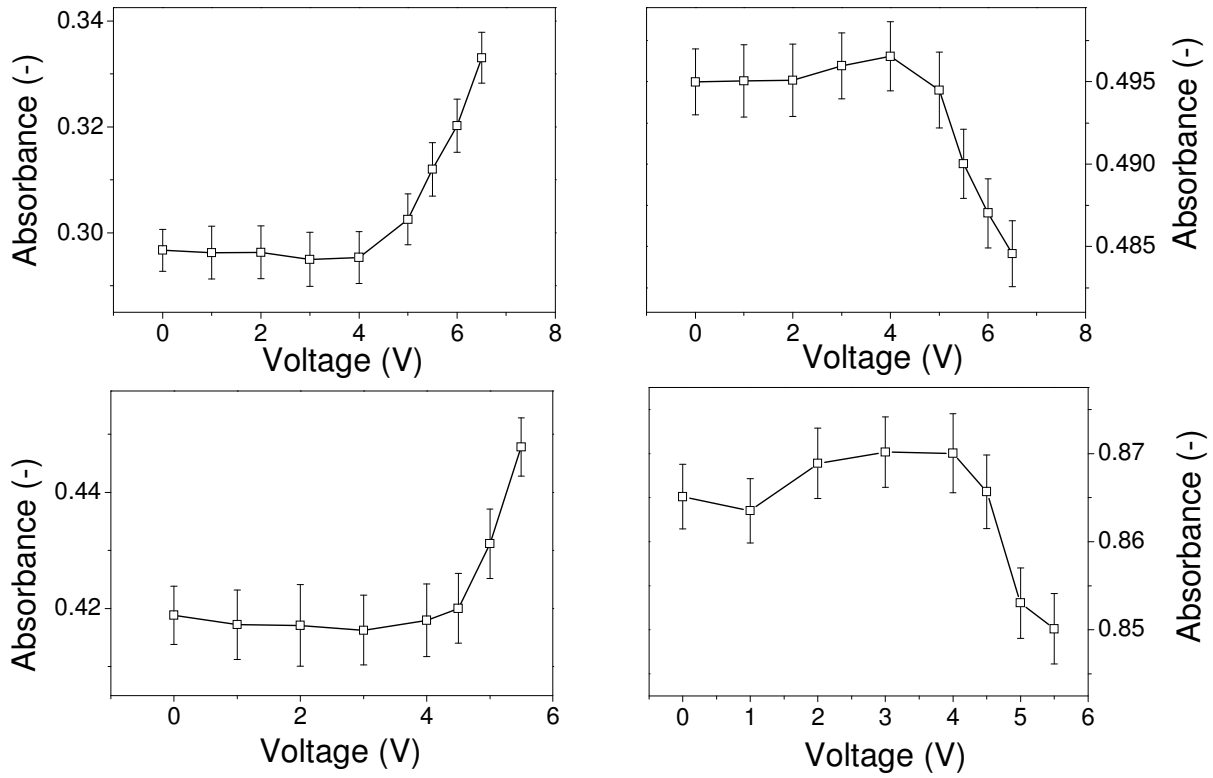


Fig. 6

**Fig. 7**

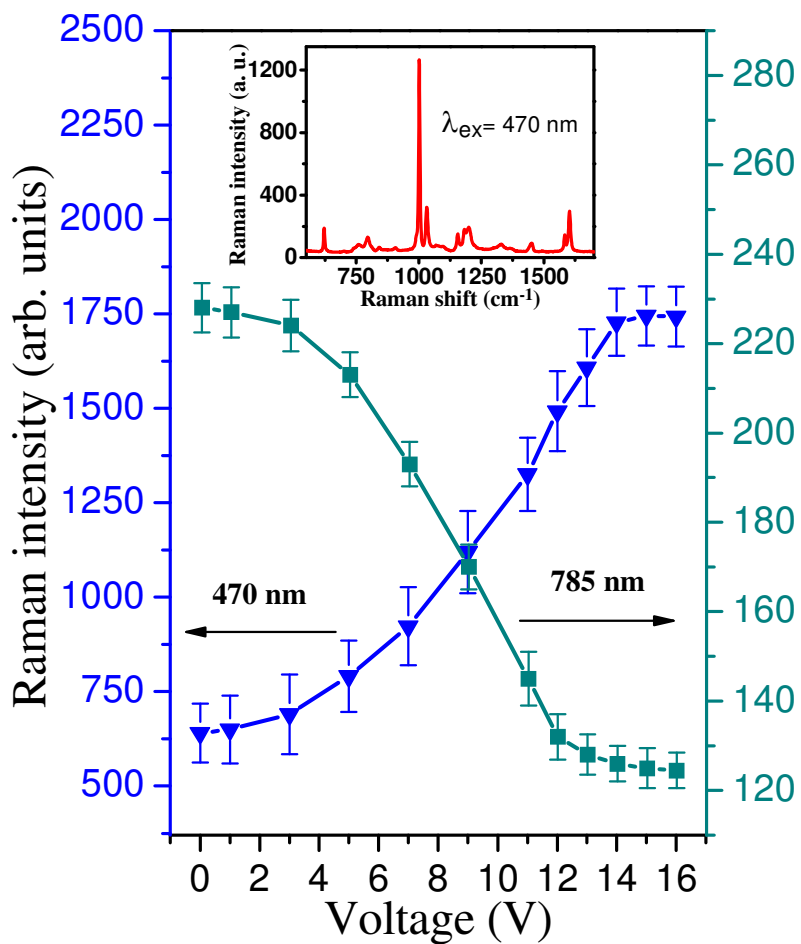
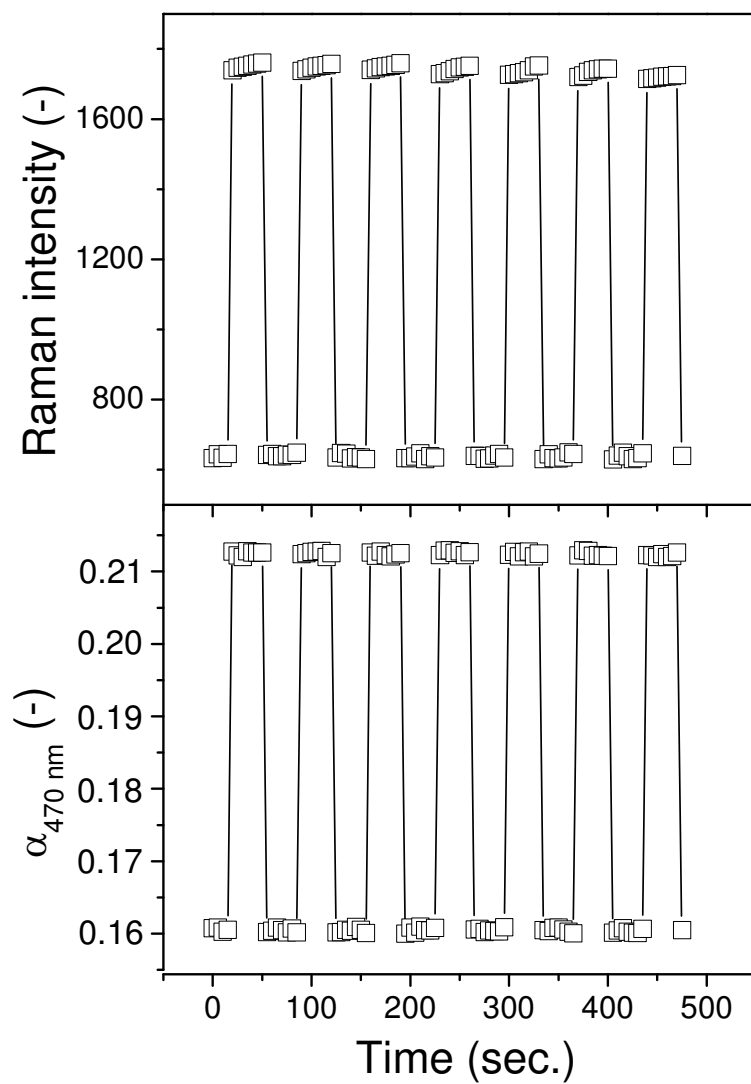


Fig. 8

**Fig. 9**